Two-axis solar tracking accomplished through small lateral translations

Justin M. Hallas,[1,2,*] Katherine A. Baker,[1] Jason H. Karp,[1,3] Eric J. Tremblay,[1,4] and Joseph E. Ford[1]

[1]Department of Electrical and Computer Engineering, University of California, San Diego, 9500 Gilman Drive, Mail Code 0409, La Jolla, California 92093, USA

[2]Pacific Integrated Energy, San Diego, California 92130, USA

[3]General Electric Global Research, Niskayuna, New York 12309, USA

[4]École Polytechnique Fédérale de Lausanne, CH-1015 Lausanne, Switzerland

*Corresponding author: jh@pienergy.com

Received 19 June 2012; accepted 9 July 2012;
posted 24 July 2012 (Doc. ID 170924); published 28 August 2012

High-concentration solar-power optics require precise two-axis tracking. The planar micro-optic solar concentrator uses a lenslet array over a planar waveguide with small reflective facets at the focal point of each lenslet to couple incident light into the waveguide. The concentrator can use conventional tracking, tilting the entire assembly, but the system geometry also allows tracking by small lateral translation of the lenslet relative to the waveguide. Here, we experimentally demonstrate such microtracking with the existing concentrator optics and present optimized optical designs for systems with higher efficiency and angle range.

OCIS codes: 350.6050, 220.1770, 350.3950, 130.2755, 040.5350, 220.4830.

1. Introduction

Conventional high-concentration photovoltaic (CPV) systems use precise mechanical trackers that rotate the concentrator to maintain alignment with the Sun [1]. These trackers usually are bulky, require a pedestal, and must be mechanically stable against wind-loading forces. They can be a sizeable fraction of the total system cost [2].

Recently, we presented the micro-optic solar concentrator shown in Fig. 1 [3]. In contrast to some other recent designs that require stepped waveguides [4,5], this waveguide is planar. Our design consists of a microlens array mounted above a planar waveguide separated by a small air-gap. The waveguide is patterned with small reflective facets located at the focal point of each lens in the array. Normally, incident light is focused by the lenses onto the facets that reflect the light into guided modes of the planar waveguide. The coupled light propagates toward an edge-mounted photovoltaic (PV) cell.

A. Lateral Translation Microtracking

The micro-optic solar concentrator can track the Sun using conventional mechanical tracking, tilting, and rotating the entire optical assembly to maintain direct normal illumination from the Sun. An alternative to tilting the entire CPV system is tracking by moving the PV device relative to a fixed lens, or by moving an array of lenses over an array of small PV cells [7]. This type of tracking can offer significant advantages over conventional tracking. These advantages include a lowered sensitivity to wind loading because of a fixed outer frame and compact form factor and have less expensive motion mechanics because of the small amount of motion required in only one plane. However, there are disadvantages to using

1559-128X/12/256117-08$15.00/0

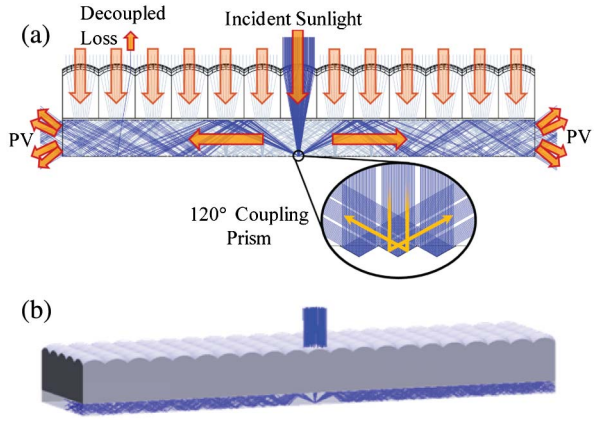

Fig. 1. (Color online) Illustration of planar micro-optic solar concentrator operation. (a) Lenslets and microprisms direct sunlight into a slab waveguide with edge-mounted PV cells and (b) perspective view with one lenslet illuminated [3,6].

a large number of small PV cells, including packaging tolerances and costs, and efficiency losses from nonuniform photocurrent from cascaded PV cells. The combination of microlenses with a waveguide allows the advantages of lens miniaturization without the costs associated with a corresponding increase in the number of PV cells.

As the incoming light tilts with respect to the planar micro-optic concentrator, the focused light begins to drift and miss the reflective facet. To recapture the light, the waveguide can be translated with respect to the lens array so that the focused light once again falls on the reflective facet, as seen in Fig. 2(c). The required lateral shift is $f \tan \theta$ where f is the focal length of the lens and θ is the angle off-axis. Because of the large segmentation of the input aperture, small focal lengths are easily achievable and, as such, only small lateral translations are required.

2. Optical Design

A. Design Requirements

The optical efficiency of this type of system is constrained by two factors: the coupling efficiency and the propagation efficiency within the waveguide. The coupling efficiency includes surface reflections, the capability of the microlenses to focus on a small spot on the back of the planar waveguide across the range of angles of interest, and the capability of the small reflective facets or "injection-features" to efficiently couple light into guided modes of the planar waveguide. This last factor must consider the incoming angular spectrum, including the numerical aperture of the microlenses. The propagation efficiency in the planar waveguide is limited by material absorption and secondary interactions with the reflective facets, which tend to decouple the light.

Solar concentrator optics are designed for the angular divergence and spectrum of the Sun. Maintaining peak operation as the Sun travels across the sky over the course of the day and the year is generally relegated to tracking mechanics; this is not the case

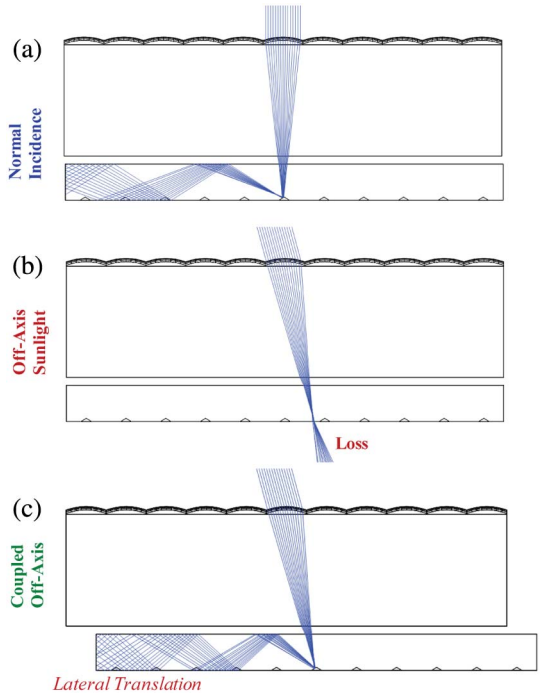

Fig. 2. (Color online) Normally incident light is focused by the lenses in the array onto reflective facets on the waveguide surface, which inject the light into guided modes (a) light that is tilted with respect to the concentrator is focused onto laterally shifted spots that miss the coupling features; (b) these spots can be recoupled by laterally translating the waveguide; and (c) lateral translation [8].

for a microtracked solar concentrator. Microtracking of a concentrator offers a decrease in the size and complexity of tracking mechanics at the cost of additional constraints on optical design.

The range of input angles required is set by the path of the Sun as well as the role of microtracking in the system. Microtracking can be utilized for both axes in a system that is mechanically fixed, primarily for one axis with a single axis gross mechanical tracker, or to relax the tolerances of a two-axis gross mechanical tracker. Microtracking of a fixed solar concentrator and one that utilizes gross mechanical polar tracking will be considered here.

Figure 3 shows a plot of the path and irradiance in San Diego (32.7° latitude) over the course of the day and year [8]. This plot was reformatted to show the peak intensity versus the angle the microlenses would see in a fixed mechanical mounting configuration in Fig. 4(b), and a gross mechanical polar-tracked configuration in Fig. 4(d). The calculations for Fig. 4 include the reduction in intensity equal to the cosine of the angle off normal that results in an effectively reduced illumination area. This reduction in intensity is especially significant for the fixed configuration. The angular requirements of the polar-tracked system folds onto the angular divergence of the Sun in one axis and the declination angle of ± 24 deg in the other axis.

B. Optical Design

The planar micro-optic solar concentrator prototype used an off-the-shelf lens array designed for on-axis

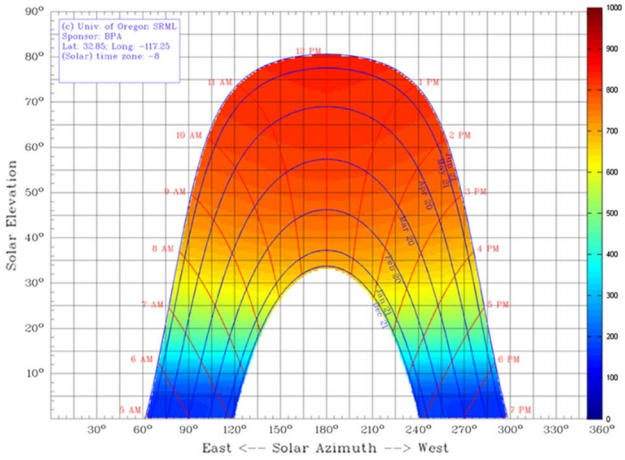

Fig. 3. (Color online) Plot of path and irradiance of Sun in San Diego over the course of a year. (Path data courtesy of University of Oregon, Solar Radiation Monitor Laboratory.)

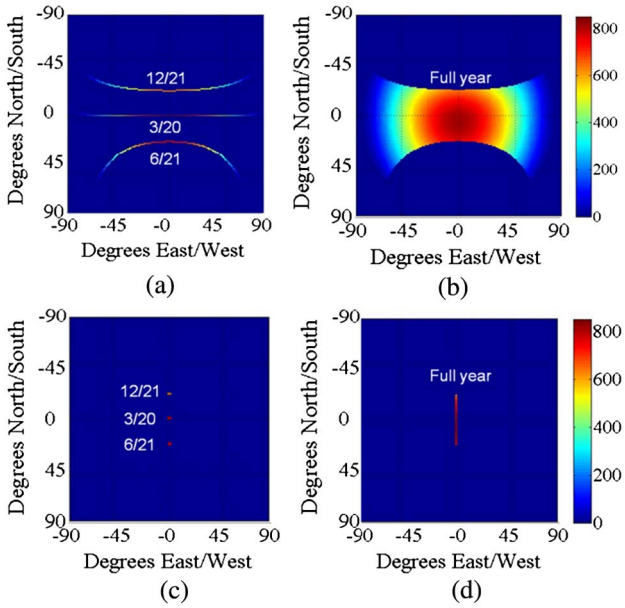

Fig. 4. (Color online) Peak intensity of sunlight as a function of angle (a) over the course of three example days and (b) over the course of a full year for a fixed flat panel tilted at latitude in San Diego, California. (c) and (d) The same are shown for a one-dimensional (1D) mechanically tracked system tilted at latitude [9,10].

illumination. Its performance suffers at any non negligible angle because of off-axis aberrations as seen in the ZEMAX simulation results in Fig. 5(a).

To meet the angular requirements for a micro-tracked system, we evaluated and optimized various lenses for small spot size over the range of angles of interest, given solar spectrum light at discrete angles, while keeping the lens aperture 1 mm wide. First, we optimized the thickness and curvature of an aspheric acrylic singlet as shown in Fig. 5(b). Although better than the lens array used in the prototype, the off-axis performance is still relatively poor.

We also examined a doublet consisting of acrylic and polycarbonate lenses as seen in Fig. 5(c). The two lenses in this pair are separated by an air-gap and are constrained to move together unlike Duerr *et al.* [7] whose system utilized two independent lens arrays. This choice sacrifices performance in exchange for a simpler control scheme. In addition, off-axis light is vignetted at the second lens, resulting in loss at angles beyond 30 deg. The performance of our doublet is superior to the singlet because of reduced aberrations, but this comes at the cost of increased manufacturing complexity as well as vignetting.

Next, we examined a different geometry: the reflective microlens seen in Fig. 5(d). The reflective microlens works well with broad-spectrum light as the optical power is less dependent on the refractive index and more dependent on the shape of the lens. The reflective microlens benefits from a small sag that should help with manufacturability. It offers similar performance to the refractive doublet without the increased manufacturing complexity. The downside of the reflective microlens is the introduction of two extra loss factors: loss related to shadowing of incoming light by the injection features and loss associated with a second metallic reflection at the reflective lens.

After the initial focusing by the lenslet, the next part of the optical system is a coupling feature that deflects the light into guided modes of the planar waveguide. The injection feature used in this system is a periodic 120 deg prism. The size of the coupling feature can be optimized for the specific lens and geometric concentration used. In the prototype system, the coupling feature diameter was 60 μm. The capability of the prism to couple light into the waveguide as a function of the angle in Fig. 6 compares well with the range of input angles incident on the system in Fig. 4(b). This, however, does not include the f-number of the lens, which increases angular divergence and results in lower efficiency at higher field angles. More complicated coupling features can be designed to limit loss because of subsequent interactions, including the use of horizontal stepping [11,12].

C. System Performance

The efficiency of the entire system was calculated by combining arrays of the microlenses with a matching array of coupling features. This was done in ZEMAX nonsequential analysis. The coupling feature size was optimized to maximize efficiency for each different configuration considered at 128× geometric concentration.

Figure 7 shows the overall system efficiency as a function of the input angle for the existing prototype and three optimized lens designs. This simulation includes the angular and wavelength spectrum of the Sun. The efficiency of the prototype singlet and optimized singlet are similar with only a slight improvement in acceptance angle. The efficiency of the refractive doublet and reflective designs are similar except that the refractive doublet works slightly

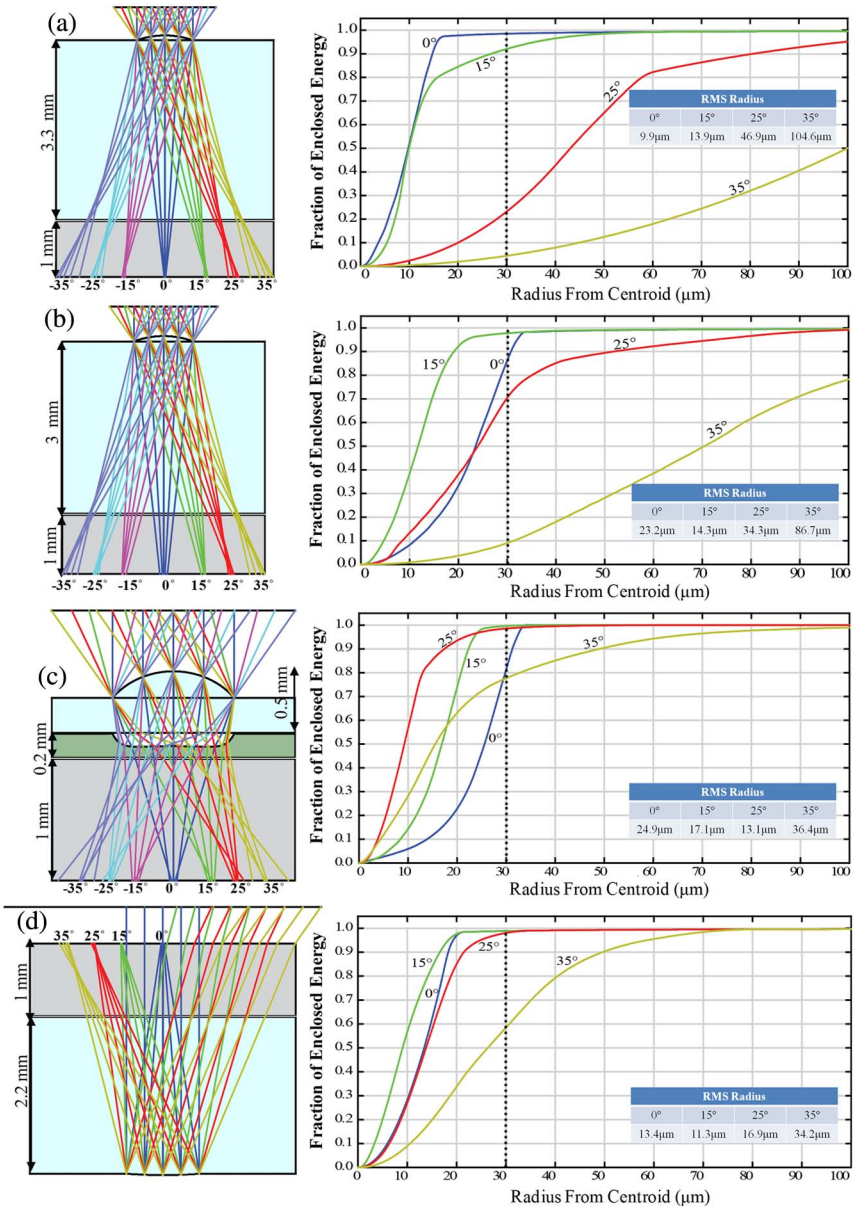

Fig. 5. (Color online) Ray-trace diagrams at discrete angles up to 35 deg using the wavelength spectrum of sunlight (left) and corresponding plots of encircled energy versus radius from centroid (right) for (a) the prototype singlet, (b) an optimized singlet, (c) a refractive doublet, and (d) a reflective lens. The dashed line at 30 μm corresponds to the radius of the coupling feature used in the prototype.

better on-axis and the reflective has a slower roll-off at higher angles. Both of these designs are limited by the coupling feature in the North-South direction, which explains the lack of rotational symmetry.

Table 1 details the annual percentage of energy delivered to the edge-mounted PVs with respect to the incident energy for an untracked panel configuration and a configuration with 1D tracking. This percentage is relative to the incident light on the panel given the tracking configuration, so a 1D mechanically tracked system receives more than twice as much energy as a static panel. From the table, the reflective design is the most promising option for a fixed system because of its larger angular acceptance, and the refractive doublet is the best design for use in conjunction with a polar tracker because of its higher on-axis efficiency.

The optical efficiency of this system with on-axis illumination has a linear relationship to concentration that is related to material absorption and secondary reflections from coupling features. Figure 8 illustrates this relationship for the three optical designs presented here. Note that the slope of the curve for the singlet is steeper as the optimum coupling feature width is larger, resulting in proportionally more propagation loss as concentration increases.

To experimentally verify the validity of the ZEMAX simulations, the planar micro-optic solar concentrator was mounted onto a rotation stage and illuminated by a Thermo Oriel xenon arc lamp solar

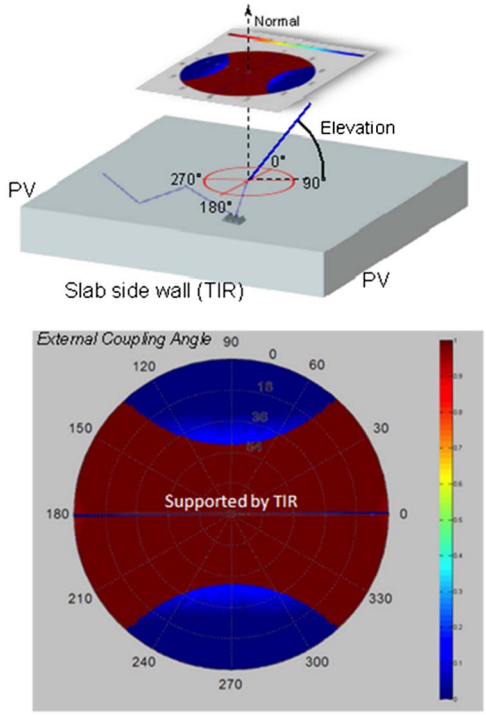

Fig. 6. (Color online) Optical coupling of light reflected from a 120 deg angled injection facet as a function of external incidence angle (including surface refraction, but not lens effects) for an F2 ($n = 1.62$) waveguide with an air cladding. The vertical–horizontal coupling asymmetry seen in the lower graph results from light reflecting from the adjacent facet and emitting from the entrance aperture [9].

simulator as seen in Fig. 9. We measured the concentrator output with an edge-mounted PV cell as the angle of the stage was swept in two orthogonal directions. As shown in Fig. 10, the experimentally

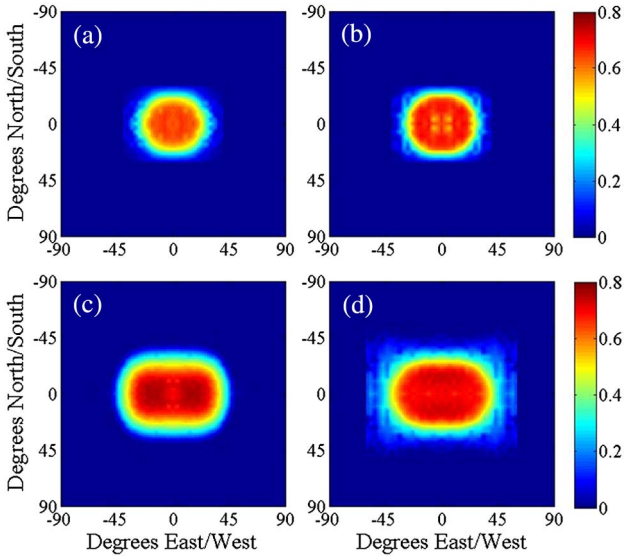

Fig. 7. (Color online) Optical efficiency as a function of angle for 128× geometric concentration for (a) the prototype, (b) the optimized singlet, (c) the optimized doublet, and (d) the reflective design.

Table 1. Annual Percentage of Energy Incident on Panel Collected for Simulated Lens Designs

	Prototype Singlet	Optimized Singlet	Doublet	Reflective
Static Panel	35%	42%	59%	65%
1D Tracking	60%	65%	75%	69%

measured values match well with the results from the ZEMAX nonsequential simulation.

3. Tracking Platform

A. Mechanical Design

To test the concept of microtracking in a manner that would accurately simulate real-world conditions without the use of expensive mechanics and with feedback, we designed and fabricated a self-contained mechanical tracking platform. The system holds the waveguide and PV fixed while allowing for small angular rotation and small-range lateral translation of the lenslets by rotating three eccentric cams held in contact with the waveguide by springs as seen in Figs. 11–13.

We achieved the required resolution for the translational motion by using a miniature stepper motor

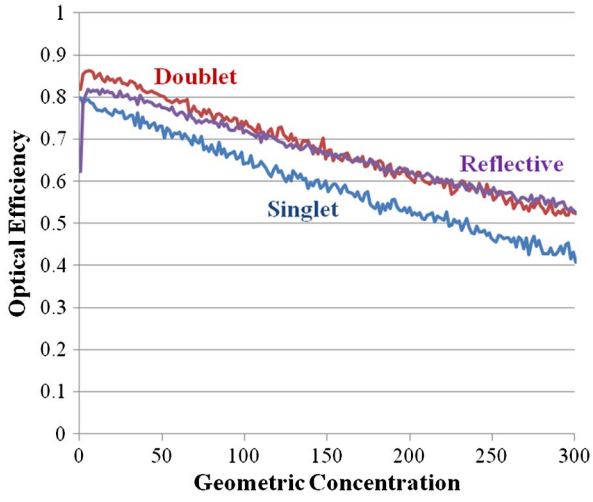

Fig. 8. (Color online) Simulated optical efficiency versus geometric concentration using the three different lens designs with coupling feature width optimized at 128× concentration illuminated by on-axis sunlight.

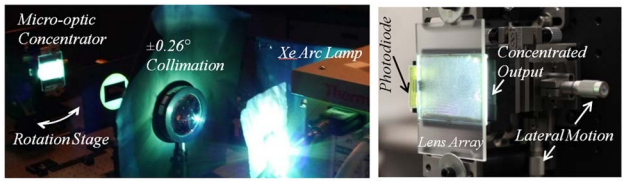

Fig. 9. (Color online) Experimental setup, including the concentrator mounted onto an alignment stage and a rotation stage illuminated by an Xe arc lamp [8].

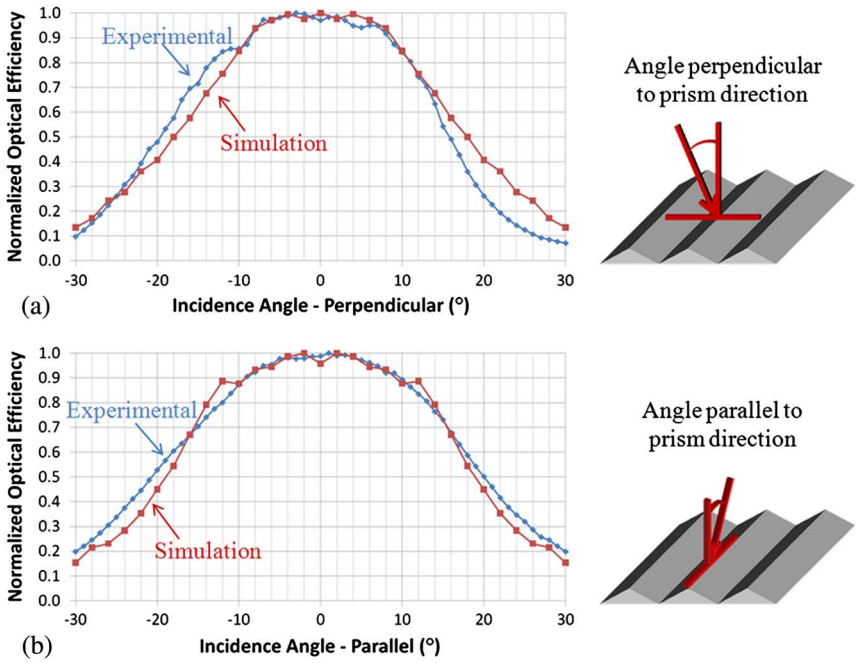

Fig. 10. (Color online) Normalized optical efficiency versus angle of incidence (a) perpendicular and (b) parallel to prism direction [6].

with 20 steps per rotation, a 64:1 gear head reduction, and a 20:1 reduction worm drive, giving a total of 25,600 steps per rotation of the eccentric cam. The decentration of the cams is 2 mm, giving a maximum total translation of 4 mm and a translation per step between −0.5 and 0.5 μm depending on the phase of the cam, which is much smaller than the 60 μm injection feature size used in our prototype. The required translation is independent of the system aperture so the same drivers would work for a 1 m × 2 m panel.

B. Electrical Control and Measurement

We used an Atmel AVR microcontroller to optimize the measured output from the PV cell by adjusting the position of the three eccentric cams. The microcontroller drove the stepper motors, which drove the cams using EasyDriver stepper motor drivers. In this prototype, we used a multijunction PV cell, but the concentrator is substantially wavelength dependent and could be used with any PV technology that allows direct access to the PV surface.

We performed initial alignment manually using push-button input to control the stepper motors. This procedure could be automated with the addition of some form of positional feedback allowing the microcontroller to detect the orientation of the eccentric cams. With positional feedback included in the system, the alignment process could be made faster and more efficient with the addition of a gyroscope or an inexpensive camera mounted behind the lens array to track the position of focused spots.

After the initial manual alignment, the microcontroller followed the Sun by rotating the cams periodically in small increments using a "hill-climbing" algorithm. In fixed intervals, the cams were stepped forward in the direction the Sun should be moving to measure the slope of the output with respect to motion. When the microcontroller detected a negative slope of the output voltage when stepping the cam

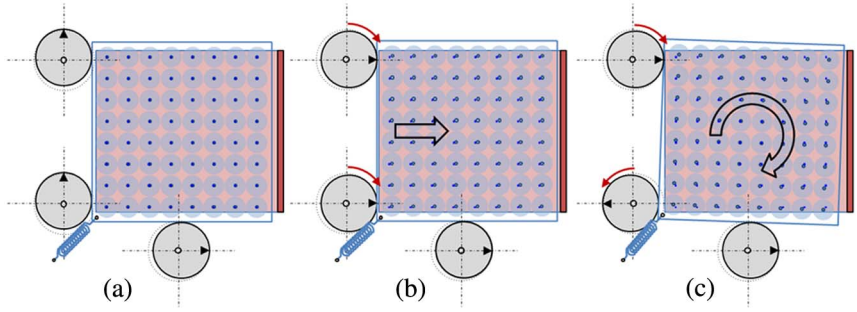

Fig. 11. (Color online) (a) Initial position of cams with lenses centered above injection elements, (b) demonstration of lateral motion with the pair of cams moving together for one axis of motion and the bottom cam providing the other axis, and (c) rotation is achieved by moving one of the two cams on the same side with respect to the other [6].

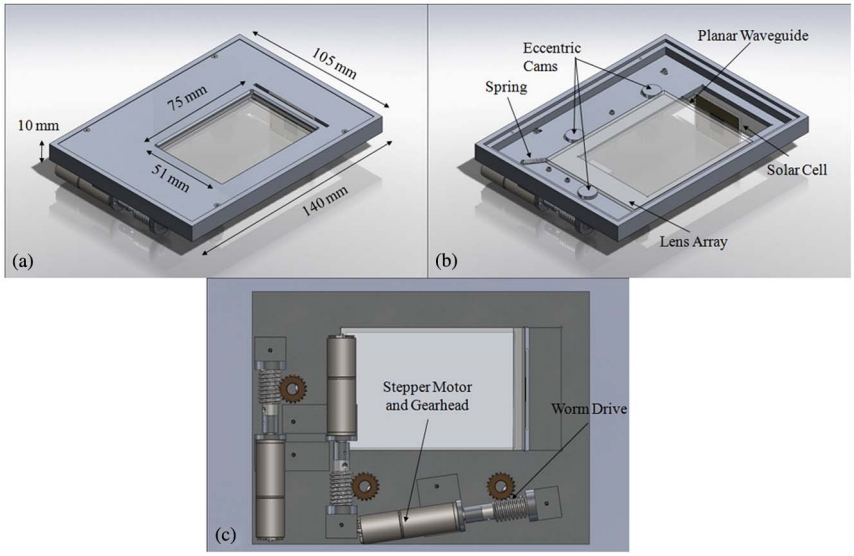

Fig. 12. (Color online) Frame and eccentric cams are made out of anodized aluminum coated in Teflon for low-friction contact with the lens array. A spring keeps the lens array in contact with the cams. (a) Top view with cover, (b) top view with cover removed, and (c) bottom view showing stepper motor mounting and worm drives [6].

forward, it stopped laterally translating in that direction. The algorithm's rate of motion was calculated based on the rate of the Sun's motion. If the algorithm that measures the slope by stepping the cams forward was run too often, the system would "outrun" the Sun and have to be reversed. In this experiment, we did not drive the cams in reverse because of the significant backlash and lack of positional feedback in this prototype. Although recovering from the backlash is trivial, it requires time in which the output is suboptimal.

Figure 14 shows the output from the system for 1 h, recorded over a serial link to a laptop from the microcontroller. The data were taken in the afternoon, on a tripod initially mechanically aligned to be normal to the Sun. The green curve is the maximum response expected calculated by multiplying the $\cos(\theta)$ losses resulting from the reduced apparent aperture size, intensity reduction caused by larger scattering in the atmosphere as the Sun goes down, and reduction in performance because of poor off-axis performance of the microlens in the prototype system. The large dips in the tracked response were due to intermittent cloud cover. After the clouds passed, the tracker recovered alignment as it was not trying to maintain some specific maximum value but instead was following the slope of the curve using a hill-climbing algorithm.

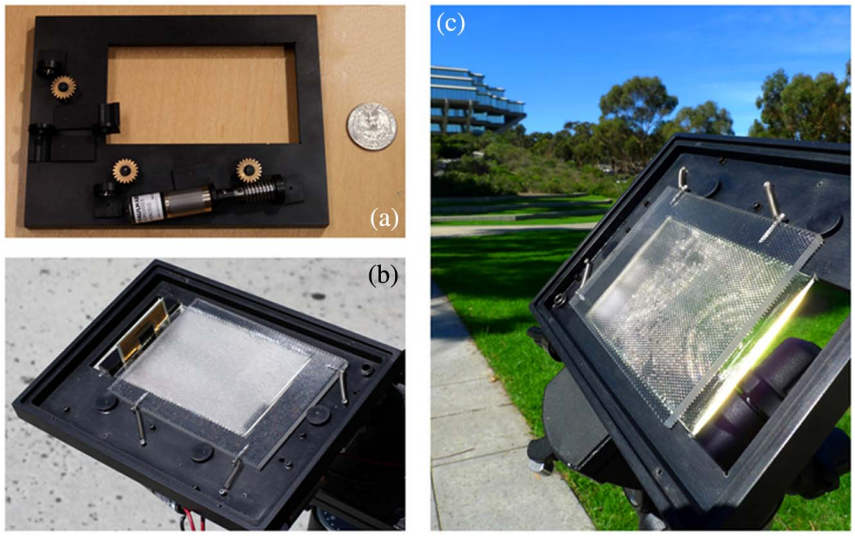

Fig. 13. (Color online) Figure showing fabricated system. (a) Bottom view of partially assembled microtracking platform, (b) top view with attached solar cell, and (c) system without solar cell demonstrating bright output [8].

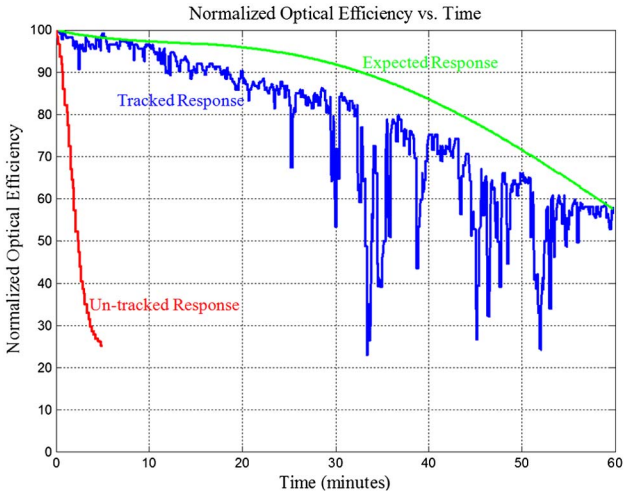

Fig. 14. (Color online) Plot of normalized optical efficiency versus time for an untracked system (red), a system that tracks the Sun using a hill-climbing algorithm (blue) and the expected response from the tracked system based on geometrical losses, intensity reduction, and off-axis performance of the system (green) [8].

4. Conclusion

We present microtracking of a planar micro-optic solar concentrator. As good off-axis optical performance of the concentrator lenslets is essential, we compared several different lens designs, including a refractive singlet and doublet as well as a reflective singlet. The reflective lens and the refractive doublet have similar performance, whereas the singlet would likely be limited to use with a polar tracker. The reflective design can collect up to 65% of incident collectable energy when mounted in a fixed frame with no gross mechanical tracking at a geometric concentration of 128×. The designed refractive doublet can collect up to 75% of incident energy when used in conjunction with a polar tracker at the same concentration. We designed and fabricated a platform to test the concept of microtracking of a planar micro-optic solar concentrator. After mounting the optics and solar cell, we added electrical feedback and control. During outdoor testing, the device successfully tracked the Sun suitably insensitive to cloud cover. The tracked response matched very closely with the expected response due to the performance of the planar micro-optic solar concentrator, the lower intensity sunlight as the Sun went down, and the $\cos(\theta)$ geometrical loss of intensity as the Sun subtended a larger angle with respect to the normal planar micro-optic solar concentrator. This type of system could potentially scale and offer the benefits of a CPV system without requiring bulky mechanical trackers.

This research was made possible by support from the National Science Foundation under Small Grants for Exploratory Research (SGER) award No. 0844274, from the California Energy Commission as part of the California Solar Energy Collaborative, and from Cognitek.

References

1. S. Kurtz, "Opportunities and challenges for development of a mature concentrating photovoltaic power industry," NREL Tech. Rep. (2010).
2. A. W. Bett and H. Lerchenmüller, "The FLATCON system from concentrix solar," in *Concentrator Photovoltaics*, A. L. Luque and V. M. Andreev, eds. (Springer, 2007).
3. J. H. Karp, E. J. Tremblay, and J. E. Ford, "Planar micro-optic solar concentrator," Opt. Express **18**, 1122–1133 (2010).
4. J. P. Morgan, "Light-guide solar panel and method of fabrication thereof," U.S. patent 7,873,257 B2 (11 June 2008).
5. S. Ghosh and D. S. Shultz, "Solar energy concentrator," U.S. patent 7,672,549 B2 (2 March 2010).
6. J. M. Hallas, J. H. Karp, E. J. Tremblay, and J. E. Ford, "Lateral translation micro-tracking of planar micro-optic solar concentrator," in Proc. SPIE **7769**, 776904 (2010).
7. F. Duerr, Y. Meuret, and H. Thienpont, "Tracking integration in concentrating photovoltaics using laterally moving optics," Opt. Express **19**, A207–A218 (2011).
8. J. M. Hallas, "Automated micro-tracking planar solar concentrators," master's thesis (University of California, San Diego, 2011).
9. K. Baker, J. Karp, E. Tremblay, J. Hallas, and J. Ford, "Reactive self-tracking solar concentrators: concept, design, and initial materials characterization," Appl. Opt. **51**, 1086–1094 (2012).
10. A. Rabl, *Active Solar Collectors and Their Applications* (Oxford University, 1985).
11. D. Moore, G. R. Schmidt, and B. Unger, "Concentrated photovoltaic stepped planar light guide," in *International Optical Design Conference*, OSA Technical Digest (CD) (Optical Society of America, 2010), paper JMB46P.
12. B. L. Unger, "Dimpled planar lightguide solar concentrators," Ph.D. dissertation (University of Rochester, 2010).